Applied Catalysis B: Environmental 182 (2016) 193–203

Contents lists available at ScienceDirect

Applied Catalysis B: Environmental

journal homepage: www.elsevier.com/locate/apcatb

Demethoxylation of guaiacol and methoxybenzenes over carbon-supported Ru–Mn catalyst

Momoko Ishikawa, Masazumi Tamura, Yoshinao Nakagawa*, Keiichi Tomishige**

Department of Applied Chemistry, School of Engineering, Tohoku University, 6-6-07 Aoba, Aramaki, Aoba-ku, Sendai 980-8579, Japan

ARTICLE INFO

Article history:
Received 12 June 2015
Received in revised form 9 August 2015
Accepted 11 September 2015
Available online 14 September 2015

Keywords:
Hydrodeoxygenation
Demethoxylation
Guaiacol
Ruthenium
Manganese oxide

ABSTRACT

Hydrodeoxygenation of methoxybenzenes such as guaiacol over Ru catalyst was studied. Guaiacol was demethoxylated and then hydrogenated over carbon black supported Ru–MnO_x catalyst (Ru–MnO_x/C) forming cyclohexanol and methanol in good yield (81% and 86%, respectively) under relatively mild conditions (433 K, H_2 1.5 MPa). Over Ru–MnO_x/C, yield of demethoxylated products (cyclohexanol and cyclohexane) was almost the same as that of methanol, suggesting that the methoxy group is eliminated by demethoxylation to form methanol. Other methoxybenzenes such as 2,6-dimethoxyphenol and anisole were also converted to demethoxylated saturated compounds such as cyclohexanol and cyclohexane. The reaction scheme was proposed where demethoxylation and total hydrogenation of aromatic ring from partially-hydrogenated adsorbed guaiacol proceeded in parallel. Lower H_2 pressure and higher reaction temperature were advantageous to demethoxylation. Addition of MnO_x species slowed down the reaction rate of total hydrogenation of aromatic ring, which increased the relative rate of the elimination of methoxy group to that of total hydrogenation before the elimination. The catalyst can be reused without significant loss of activity. The nanoparticles of Ru and Mn were highly dispersed, and the state of Mn species on Ru–MnO_x/C during the reaction was weakly basic MnO.

1. Introduction

Conversion of renewable biomass-related raw materials into chemicals and fuels, biorefinery, becomes more and more important [1–4]. Lignocellulosic biomass is one of the promising resources, which still remain untouched in large amount. Rapid pyrolysis of lignocellulosic biomass produces liquid called bio-oil which contains methoxybenzenes with OH, CHO and/or alkyl substituents [1,5,6]. These methoxybenzenes are derived from lignin and can also be produced by lignin pyrolysis [7–9]. These methoxybenzenes have great potentials as feedstocks for chemicals with C6 ring, and therefore transformation of these lignin-related methoxybenzenes has attracted much attention.

Hydrodeoxygenation is an effective way to transform biomass-related compounds such as polyols [10–12], furans [13,14] and phenolics [15,16] into valuable compounds which have lower oxygen contents than biomass. Guaiacol is a simple lignin-derived monomer with three different C—O bonds ((1) $C_{aromatic}$–OH, (2) $C_{aromatic}$–OC_{methyl}, (3) C_{methyl}–$OC_{aromatic}$; Fig. 1) which many lignin-derived compounds also possess. In addition, guaiacol and 4-alkylguaiacols themselves are major components of bio-oil. Therefore, hydrodeoxygenation of guaiacol is an important model reaction and has been intensively investigated [17–53]. The possible products from guaiacol reduction are shown in Fig. 2. Reported systems for hydrodeoxygenation of lignin-derived monomer include those with conventional CoMoS and NiMoS catalysts under severe conditions (typically ≥573 K) [17–21]. Metal phosphate catalysts [22,23], metal carbide catalysts [24], molybdenum-based catalysts [24–28], vanadium [29], iron [8,30], nickel [31–35], copper [36], cobalt [37], rhenium [38], and various noble metal catalysts (Pd [30,39,40], Pt [41–47], Ru [48–51] and Rh [52,53]) have been also tested by a number of groups at a similar high reaction temperature or high hydrogen pressure. Because of the order of bond dissociation energy of the three bonds ((1)>(2)>(3)) [17,30,32] and the better accessibility of the bond (3), many reported systems are considered to dissociate the O—CH_3 bond of guaiacol at first to give catechol (demethylation) [22,23,33,44,45]. The methyl fragment is usually transformed into methane, while in some systems transalkylation procceds to give methyl-substituted ring products such as toluene, methylcatechol and cresol [22,44,45,48]. The produced catechol was converted to mono-oxygenated compounds such as phenol and then hydrocarbons such as benzene. Generally, acids can assist the dissociation of C—O bonds as well as alkylation of benzene ring, and many systems

* Corresponding author. Fax: +81 22 795 7215.
** Corresponding author. Fax: +81 22 795 7214.
E-mail addresses: yoshinao@erec.che.tohoku.ac.jp (Y. Nakagawa), tomi@erec.che.tohoku.ac.jp (K. Tomishige).

http://dx.doi.org/10.1016/j.apcatb.2015.09.021
0926-3373/

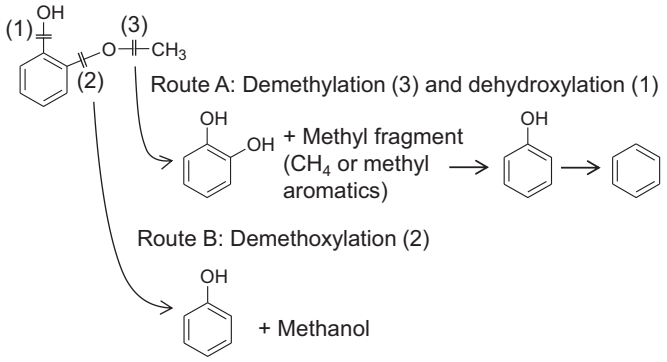

Fig. 1. Dissociation of C—O bonds in guaiacol.

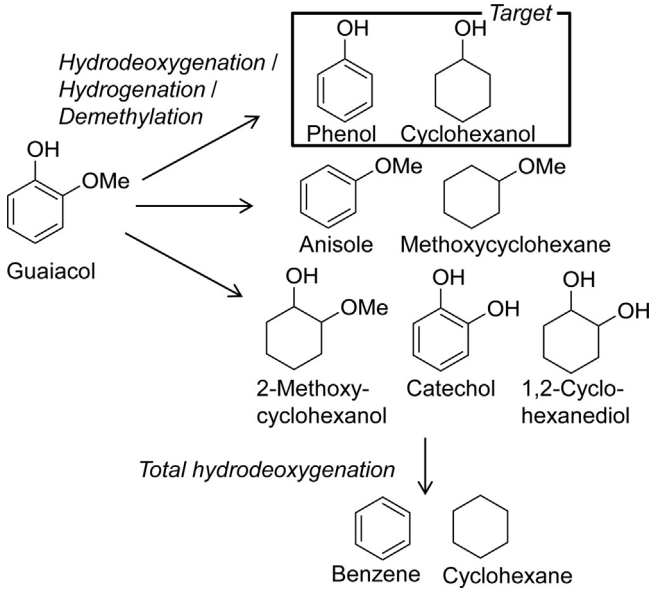

Fig. 2. Possible products from guaiacol reduction.

use acid as one of catalyst components. However, with this route ("Route A" in Fig. 1) the selective productions of mono-oxygenated compounds (phenol, cyclohexanone and cyclohexanol), which are more valuable than hydrocarbons (benzene and cyclohexane), are difficult because both catechol and phenol have similar phenolic OH groups (type (1) bonds). In fact, most literature studies focused on the production of hydrocarbons. High yield of mono-oxygenated compounds was only obtained at specific reaction time, and the highest yields were around 80% [26,30,36,38,50]. On the other hand, the preferable dissociation of type (2) bond (demethoxylation) to that of type (3) can selectively give mono-oxygenated compounds with one OH group ("Route B" in Fig. 1). In addition, the removed methyl group is converted to methanol, which is more valuable than methane.

Our group has very recently reported a catalyst system with combination of commercial active-carbon-supported Ru catalyst (denoted as c-Ru/AC) and MgO for demethoxylation of guaiacol at relative lower temperature, 433 K [49]. The main products are cyclohexanol and methanol. Among commercial active-carbon-supported noble metal catalysts, Ru showed the highest selectivity to cyclohexanol. Sels et al. have very recently reported Ni/CeO_2-catalyzed alkylguaiacol reduction to alkylcyclohexanol [34]. The use of basic material (MgO, CeO_2) is in contrast to other literature systems where acidic supports were sometimes used. In our system, demethylation reaction is suppressed by addition of basic MgO. Observed by-products were 2-methoxycyclohexanol, cyclohexane and methane which are formed by hydrogenation of guaiacol, hydrodeoxygenation of cyclohexanol and hydrodeoxygenation of methanol, respectively. Although these side-reactions were suppressed to some extent by MgO addition, there is still room for improvement in yields of cyclohexanol and methanol (~80% over c-Ru/AC + MgO). In addition, it was a problem that MgO was not stable during the reaction in the presence of water solvent and acidic substrate. Furthermore, demethoxylation proceeds only when a phenolic OH group is also present in the substrate: In the case of anisole or dimethoxybenzene, the simple hydrogenation to methoxycyclohexane and dimethoxycyclohexane, respectively, was the main reaction, and demethoxylation hardly proceeded.

Herein, we report an easy-to-handle demethoxylation catalyst, namely Ru–MnO_x/C. This catalyst gives cyclohexanol and cyclohexane from guaiacol and anisole, respectively, in higher yield than c-Ru/AC + MgO. The yield of methanol is also higher. The factors which control the selectivity were discussed such as hydrogenation activity and acidity/basicity of the catalyst.

2. Experimental

2.1. Catalyst preparation

The commercial active-carbon-supported Ru catalyst (Ru = 5 wt%) was purchased from Wako (denoted as c-Ru/AC). Ru catalysts on various supports were prepared by impregnation method using aqueous $Ru(NO)(NO_3)_3$ (Strem Chemicals) as a precursor. The carbon black (Vulcan-XC72, Cabot Corporation Ltd., BET surface area 254 m^2/g; denoted as C), active carbon (Shirasagi FAC-10 (Japan EnviroChemicals, Ltd., 851 m^2/g; denoted as AC)), SiO_2 (Fuji Silysia G-6, calcined at 973 K for 1 h, 535 m^2/g), AlOOH (Wako, as-received, 169 m^2/g), TiO_2 (Nippon Aerosil P25, calcined at 973 K for 1 h, 25 m^2/g), MnO_x (prepared by precipitation method using $Mn(NO_3)_2$ and Na_2CO_3; calcined at 773 K for 5 h, 18 m^2/g) and ZrO_2 (Soekawa Chemical, calcined at 973 K for 1 h, 31 m^2/g) were used as supports. Loading amount of Ru was 5 wt%. Ru–M/C and Ru–MO_x/C (Ru = 5 wt%; M = Mn, Fe, Co, Ni, Cu, Zn, Rh, Pd, Pt) were prepared by co-impregnation method using mixed aqueous solution of metal precursors. MnO_x/C (Mn = 5 wt%) was also prepared by impregnation method. Used precursors were $Ru(NO)(NO_3)_3$, $Mn(NO_3)_2{\cdot}6H_2O$, $Fe(NO_3)_3{\cdot}9H_2O$, $Co(NO_3)_2{\cdot}6H_2O$, $Ni(NO_3)_2{\cdot}6H_2O$, $Cu(NO_3)_2{\cdot}3H_2O$, $Zn(NO_3)_2{\cdot}6H_2O$, $Rh(NO_3)_3$, $Pd(NO_3)_2$ and $Pt(NH_3)_4Cl_2{\cdot}H_2O$. The loading amount of M was represented by the molar ratio of the additive to Ru. After impregnation, all the catalysts were dried at 383 K overnight, and heated under N_2 at 573 K for 1 h. MnO (Strem Chemicals), Mn_2O_3 (Strem Chemicals) and MnO_2 (Wako) were used as received and MgO (UBE 500A) was used after calcination at 973 K for 1 h.

2.2. Activity tests

Hydrodeoxygenation of guaiacol was performed in a 190-ml stainless-steel autoclave with an inserted glass vessel. The catalyst, guaiacol (substrate) and water (solvent) were put into the autoclave (typical amount: 0.05 g, 0.5 g and 10 g, respectively) together with a spinner. After sealing the reactor, the air content was purged by flushing three times with 1 MPa hydrogen (99.99%; Nippon Peroxide Co., Ltd.). The autoclave was then heated to the reaction temperature, and the temperature was monitored using a thermocouple inserted in the autoclave. The catalyst was reduced during the heating, which typically took about 45 min. Then the hydrogen pressure was increased to the intended value. During the experiment, stirring rate was fixed at 250 rpm. After an appropriate reaction time, the reactor was cooled down and the gases were collected in a gas bag. The autoclave contents were diluted with

ethanol containing 1,4-dioxane as an internal standard. The mixed solution was transferred to a vial, while the catalyst was separated by centrifugation and filtration. Analyses were conducted with GC and GC–MS with TC-WAX or Rtx-1-PONA capillary column. Yields and selectivities were calculated based on the number of C6 rings in the substrate and products excepted for C1 products (methanol and methane). The difference in the mass balance was always in the range of experimental error (±5%). Yield of methanol and methane were calculated from the total amount of methoxy groups in the substrate: [(amount of produced methane or methanol/mol)/{(amount of loaded substrate/mol)×n}]×100 (%); n = 1 for guaiacol, n = 2 for 2,6-dimethoxyphenol. In some cases the sum yield of methanol, methane and products with a methoxy group exceeded 100% because of the methane formation via cracking reaction of C6 ring.

The method of catalyst reuse was as follows: The reaction was carried out in multiple autoclaves at one time under the same reaction conditions. The catalyst after the use was collected by filtration, washed by ethanol and dried at room temperature for 12 h. The loss of catalyst during the recovery process was compensated by decreasing the number of autoclaves used in the next run. The amount of eluted metal into the reaction solution was analyzed by inductively-coupled plasma atomic emission spectrometry (ICP-AES, Thermo Fisher Scientific iCAP 6500).

2.3. Catalyst characterization

The amount of CO chemisorption was measured in a high-vacuum system by a volumetric method. The catalyst (0.1 g) in the measurement cell was reduced under H_2 flowing at 473 K for 1 h. After cooling to room temperature, CO was introduced and adsorption amount was measured. The pressure at adsorption equilibrium was about 1 kPa. The physisorption amount of CO on the support was determined by repeating the adsorption measurement after evacuation at room temperature. The chemisorption amount of CO was determined by subtracting the amount of CO in the physisorption from that in the first measurement. In the calculation of the dispersion of Ru, one surface Ru atom was assumed to adsorb one CO molecule (CO/Ru_s = 1) [54]. We ignored the adsorption of CO on MnO_x species, according to the literature [55].

Temperature-programmed reduction (TPR) was carried out in a fixed-bed flow reactor. The amount of catalyst was 0.05 g. The TPR profile of each sample was recorded from room temperature to 1123 K at a heating rate of 10 K/min under 5% H_2/Ar flow (30 ml/min). The amount of H_2 in the effluent gas after passing through a frozen acetone trap was monitored using a thermal conductivity detector.

TEM images were taken with HITACHI HD-2700. The catalysts after reduction under H_2 flow (30 ml/min) at 473 K were used as samples for the TEM observation. Supersonic waves dispersed the sample in ethanol. The samples were placed on Cu microgrids for TEM under air atmosphere.

X-ray diffraction (XRD) patterns were recorded by a Rigaku MiniFlex 600 diffractometer. Cu Kα (λ = 0.154 nm, 40 kV, 15 mA) radiation was used as an X-ray source. The samples were reduced under H_2 flow (30 ml/min) at 473 K before measurement for fresh catalysts.

Temperature programed desorption of CO_2 (CO_2–TPD) was performed in a fixed-bed flow reactor with a Q-MS spectrometer (Canon ANELVA M-201 GA-DM) as a detector. Catalysts were reduced under H_2 flow at 473 K for 1 h, and then flowing CO_2 (20 ml/min) was supplied for 10 min. The TPD profile of each sample (0.1 g) was recorded from room temperature to 1073 K at a heating rate of 5 K/min under He flow (30 ml/min).

The X-ray absorption spectroscopy (XAS) was carried out at the BL01B1 station at SPring-8 with the approval of the Japan Synchrotron Radiation Research Institute (JASRI; Proposal no. 2014A1119). The storage ring was operated at 8 GeV, and a Si (1 1 1) single crystal was used to obtain a monochromatic X-ray beam. Two ion chambers for I_0 and I were filled with 100% N_2 and 85% N_2 + 15% Ar, respectively, for Mn K-edge measurement. Both chambers were filled with 100% Ar for Ru K-edge measurement. We prepared the sample after the reduction and the catalytic use as follows. The catalyst reduction was carried out at 473 K with H_2 for 1 h in a closed circulating vacuum system, and the sample was transferred to the measurement cell without exposing to air using a glove bag filled with nitrogen. For used samples, the catalytic reaction was carried out in an autoclave. The reaction conditions were optimized to those where the substrate was totally converted. After cooling, the wet catalyst powder was transferred to the measurement cell in a glove bag filled with nitrogen. The thickness of the cell filled with the powder was 1 cm to give an edge jump of 0.6–1.8 and 0.6–2.2 for Mn K-edge and Ru K-edge measurement, respectively. The extended X-ray adsorption fine structure (EXAFS) data were collected in a transmission mode. For EXAFS analysis, the oscillation was first extracted from the EXAFS data using a spline smoothing method [56]. Fourier transformation of the k^3-weighted EXAFS oscillation from the k space to the r space was performed to obtain a radial distribution function. The inversely Fourier filtered data were analyzed using a usual curve fitting method [57,58]. For curve fitting analysis, the empirical phase shift and amplitude functions for the Ru—Ru bond were extracted from data for Ru metal. Analyses of EXAFS data were performed using a computer program (REX2000, ver. 2.6; Rigaku Corp.). Error bars for each parameter were estimated by stepping each parameter, while optimizing the other parameters, until the residual factor becomes two times as its minimum value [59]. In the analysis of X-ray adsorption near edge structure (XANES) spectra, the raw data were normalized by the edge height.

3. Results and discussion

3.1. Catalyst optimization for demethoxylation of guaiacol

First, we investigated the effect of supports for Ru catalysts without additives in hydrodeoxygenation of guaiacol (Table 1). The reaction time was set to 0.5 h or 2 h. The activities of catalysts can be compared by the reaction at 0.5 h, and the selectivities at complete conversion can be compared at 2 h. As shown in the previous report [49] and shown later, the change in the selectivities after complete conversion of guaiacol is relatively slow except those of C1 products. Both hydrodeoxygenation and hydrogenation reactions proceeded, and the main products from benzene ring were cyclohexanol, cyclohexane and 2-methoxycyclohexanol over all the catalysts. Phenol, which is a precursor of cyclohexanol, was detected in shorter reaction time (0.5 h). Regarding the C1 products, the yield of methanol was always higher than that of methane, indicating that demethoxylation is the major hydrodeoxygenation route in comparison with demethylation and dehydroxylation route over these Ru catalysts. Ru/C (supported on carbon black) showed relatively higher selectivity to cyclohexanol, and the ratio of methanol / methane was also relatively high (entries 1 (83% conv.) and 2 (>99% conv.)). Commercial Ru catalyst (c-Ru/AC) gave cyclohexanol with slightly lower selectivity than Ru/C catalyst (entries 3 (95% conv.) and 4 (>99% conv.)); however, large amount of methane was formed at longer reaction time probably by hydrocracking reaction (entry 4). The selectivity to cyclohexane was also higher than that over Ru/C. Over the home-made active-carbon supported catalyst (Ru/AC; entries 5 and 6), the selectivities to cyclohexane were similar to that over c-Ru/AC (~10%) and higher than that over Ru/C (~5%), while

Table 1
Hydrodeoxygenation of guaiacol over Ru catalysts with various supports.

Entry	Catalyst	D^a (%)	Time (h)	Conv. (%)	Selectivity (%)					Yield of C1 products (%)	
					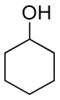	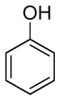		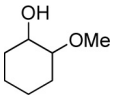	Others	Methanol	Methane
1	Ru/C	49	0.5	83	71	3	4	17	5	72	1
2			2	>99	72	<1	5	21	<1	75	4
3	c-Ru/AC	44	0.5	95	62	3	9	18	8	72	1
4			2	>99	66	<1	10	19	1,2-Cyclohexanediol 4	70	38
5	Ru/AC	56	0.5	70	61	8	6	19	6	53	<1
6			2	>99	70	<1	12	17	<1	80	5
7	Ru/SiO_2	51	0.5	63	60	4	3	19	Cyclohexanone 7, others 7	46	2
8			2	>99	71	<1	9	18	<1	71	14
9	Ru/TiO_2	42	0.5	69	57	6	2	26	9	47	1
10			2	>99	68	<1	9	21	1	70	9
11	Ru/ZrO_2	56	0.5	72	59	3	2	29	7	48	1
12			2	>99	64	<1	7	28	1	62	9
13	Ru/AlOOH	63	0.5	48	46	11	6	12	Cyclohexanone 20, others 5	39	1
14			2	98	78	<1	4	14	3	79	6

Note: Reaction conditions: guaiacol (0.5 g), catalyst (Ru = 5 wt%; 50 mg), water (10 g), H_2 (1.5 MPa), 433 K. c-Ru/AC: commercial catalyst; C: carbon black; AC: active carbon.
[a] *D*: Dispersion = $\left[\frac{\text{Amount of CO adsorption}}{\text{Total amount of Ru}}\right]$.

the yield of methane at the complete guaiacol conversion was much lower than that over c-Ru/AC. We also prepared two other active-carbon-supported catalysts, and the performances of three active-carbon-supported catalysts were almost the same (Table S1). The selectivities to 2-methoxycyclohexanol were almost the same (~20% at both incomplete and complete conversions) in all the catalysts over carbon-based supports. After all, carbon black (C) support is effective in suppressing the cyclohexane formation in comparison with active carbon supports. Ru/C catalyst seems to have lower activity in methane formation than c-Ru/AC, and this point will be confirmed later (Section 3.4). Over oxide-supported catalysts (entries 11–18), the conversion rates were lower than that over Ru/C, even when the dispersion of Ru was considered (0.5 h reactions). Oxide-supported Ru catalysts were unfavorable compared to Ru/C in view of suppressing methane formation as shown by the higher methane yields at 2 h in spite of the lower activities in guaiacol conversion than Ru/C. The ratio of the sum of hydrodeoxygenation products (cyclohexanol, phenol and cyclohexane) to the hydrogenation product (2-methoxycyclohexanol) was almost independent of reaction time and varied between supports: Ru/AlOOH > Ru/SiO_2~Ru/C > Ru/TiO_2 > Ru/ZrO_2. The catalyst with lower activity in guaiacol conversion tended to have higher selectivity to hydrodeoxygenation products. Considering the activity and selectivity, we selected carbon black (C) as the support in the following study.

Next, the Ru/C catalyst was modified by further loading of secondary metals. The modification of noble metal catalysts with secondary metals is often effective in improving the hydrodeoxygenation performances [60–67]. The performance of catalysts (molar ratio of secondary metal to Ru = 0.25) is summarized in Table 2 (2 h reactions) and Table S2 (0.5 h reactions). Ru–MnO_x/C (entry 2) catalyst showed higher selectivity to cyclohexanol than monometallic Ru catalysts and the other bimetallic catalysts, although the activity in guaiacol conversion of Ru–MnO_x/C was rather low (Table S2). Selectivity to 2-methoxycyclohexanol was decreased by addition of Mn species, and the amount of methane formation remained small. The addition of other first-row transition metal or Rh did not suppress the formation of 2-methoxycyclohexanol (entries 3–8). The addition of Pd or Pt decreased the selectivity to 2-methoxycyclohexanol; however, formation of cyclohexane was significantly promoted (entries 9 and 10). The formation of methane was promoted when Fe or Pt was added (entries 3 and 10).

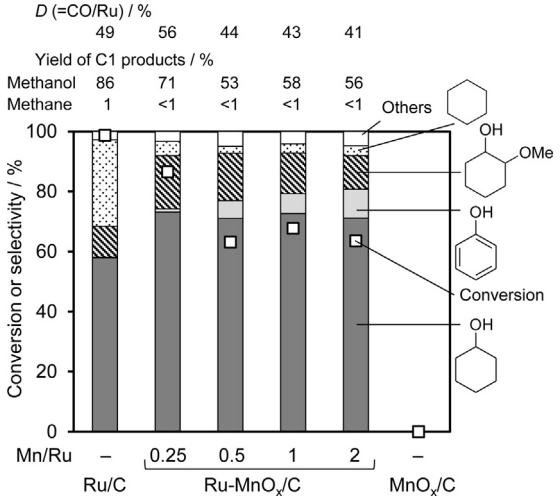

Fig. 3. Hydrodeoxygenation of guaiacol over Ru and Mn catalyst. Reaction conditions: guaiacol (0.5 g), catalyst (Metal = 5 wt%; 20 mg), water (10 g), H_2 (1.5 MPa), 433 K, 2 h. D: Dispersion calculated from CO adsorption.

We further investigated the effect of Mn loading amount (Fig. 3). The sum of the selectivity to cyclohexanol and phenol which is an intermediate of cyclohexanol formation was gradually improved by the increase of Mn amount, while the activity in guaiacol conversion was slightly decreased. Although the number of surface Ru site determined by CO adsorption was kept high in Mn-modified catalysts (CO/Ru > 0.4), small amount of Mn species may be present on the Ru particles to affect the activity of the Ru site. However, the use of Ru–MnO_x/C (Mn/Ru = 2) changed the color of the reaction solution into brown–orange from colorless, showing the apparent leaching of metal species. So we selected Mn/Ru = 1 for this study. It was confirmed the MnO_x/C had no activity in these reaction conditions.

3.2. Performance of Ru–MnO_x/C (Mn/Ru = 1)

Fig. 4 shows the time course of hydrodeoxygenation of guaiacol over Ru–MnO_x/C. The conversion at 0 h means that by the reaction during the heating. Phenol was detected in short reaction time (0–1 h). The selectivity to phenol decreased with guaiacol conversion and cyclohexanol production. These phenomena were

Table 2
Hydrodeoxygenation of guaiacol over Ru–M/C (Ru–MO_x/C) catalysts.

Entry	M	Conv. (%)	Selectivity (%)					Yield of C1 products (%)	
			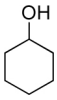	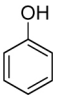		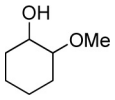	Others	Methanol	Methane
1	None	>99	72	<1	5	21	<1	75	4
2	Mn	>99	79	<1	4	16	1	84	4
3	Fe	95	73	<1	4	22	1	74	12
4	Co	>99	69	<1	6	22	3	73	2
5	Ni	>99	68	<1	5	25	2	72	2
6	Cu	>99	71	<1	5	22	2	77	3
7	Zn	78	64	2	7	24	3	55	<1
8	Rh	>99	66	<1	6	27	1	71	3
9	Pd	>99	74	<1	10	15	1	75	5
10	Pt	>99	68	<1	13	17	2	78	10

Note: Reaction conditions: guaiacol (0.5 g), catalyst (carbon black support, Ru = 5 wt%, M/Ru = 0.25; 50 mg), water (10 g), H_2 (1.5 MPa), 433 K, 2 h.

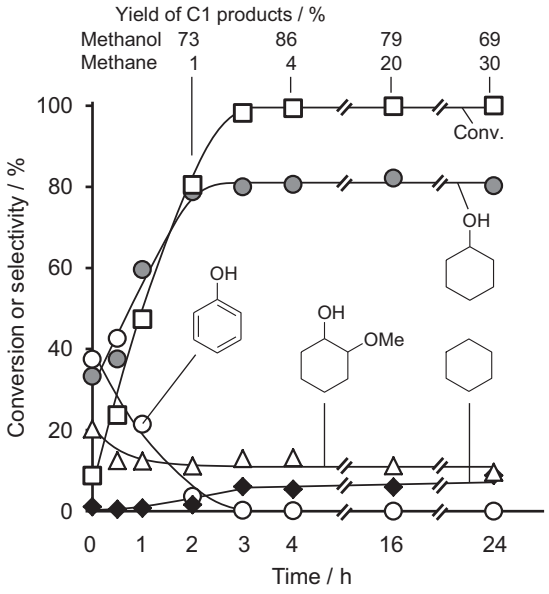

Fig. 4. Time course of hydrodeoxygenation of guaiacol over Ru–MnO_x/C (Ru = 5 wt%, Mn/Ru = 1). Reaction conditions: guaiacol (0.5 g), Ru–MnO_x/C (50 mg), water (10 g), H_2 (1.5 MPa), 433 K.

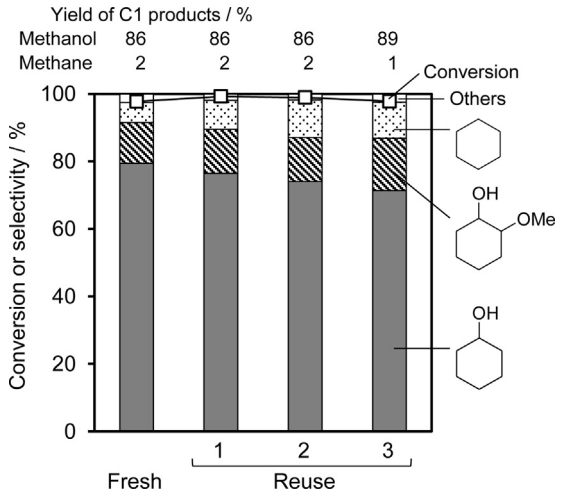

Fig. 5. Reuse experiment of Ru–MnO_x/C catalyst. Reaction conditions: guaiacol (0.5 g), Ru–MnO_x/C (Mn/Ru = 1; 50 mg), water (10 g), H_2 (1.5 MPa), 433 K, 2.5 h.

the same as observed in c-Ru/AC + MgO system [49] and indicate that phenol was the intermediate of cyclohexanol formation. After guaiacol was totally converted, selectivities to all products including C1 products were little changed, indicating that over-hydrodeoxygenation hardly occurs over Ru–MnO_x/C. The highest yield of cyclohexanol and methanol were 81% and 86%, respectively, which were achieved at 4 h. These values were higher than those of the c-Ru/AC + MgO system, where the yields of cyclohexanol and methanol were 81% and 72 %, respectively [49]. The pH values of the reaction mixture before and after the reactions showed that the reaction proceeded under weakly basic conditions (pH 7–8). The amount of metal elution during the reaction was measured by ICP-AES analysis (Table S3). Some amount of metal was eluted during the reaction in short reaction time (Ru: ~1%, Mn: ~6% of each loaded metal). The amount of eluted metal was decreased as the guaiacol converted and became below the detection limit at the total conversion of guaiacol (reaction time 4 h in Fig. 4). The elution can be due to the acidic substrate and intermediates. When acidic phenolic compounds are totally hydrogenated to neutral alcohols, eluted metals may well return to the solid catalyst.

The reuse experiment was conducted to see the stability of the catalyst. The used catalysts were collected by filtration, washed with ethanol, dried and reused for another catalytic run. The reaction time was set to 2.5 h, when guaiacol is just completely converted, to avoid the influences of metal leaching and unreacted guaiacol from former catalytic runs. The results are shown in Fig. 5. The activity of the catalyst in guaiacol conversion was not changed by reuses, and the used catalyst showed almost the same product distributions as the fresh one. The slight change in selectivity may be due to the decreasing interaction between Ru and MnO_x during leaching and re-precipitation cycle of metal species. In our previous work [49], there was difficulty on handling the c-Ru/AC + MgO catalysts in the reuse experiment, because MgO powder was transformed into muddy material due to water solvent and acidic compounds. The used Ru–MnO_x/C maintained the powdery form, so the reusability of the catalyst is considerably improved compared to the c-Ru/AC + MgO system. Therefore Ru–MnO_x/C is a better catalyst than c-Ru/AC + MgO in terms of both reusability and yield of the products.

Ru–MnO_x/C was applied to various lignin-related methoxybenzenes (Table 3). Guaiacol and 3-methoxyphenol were converted to cyclohexanol in good yield (entries 1 and 2). 4-Methoxyphenol was converted to cyclohexanol although the yield was lower (entry 3). 2,6-Dimethoxyphenol, which is also an important motif of bio-oil and lignin-derived monomers, was also converted to cyclohexanol in good yield by removal of both methoxy groups (entry 4). The

Table 3
Hydrodeoxygenation of methoxybenzenes over Ru–MnO_x/C.

Entry	Substrate	Time (h)	Conv. (%)	Products (Selectivity (%))	Yield of C1 products (%)	
					Methanol	Methane
1	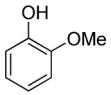	4	>99	 (81), 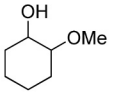 (13),  (5), Others (1)	86	4
2	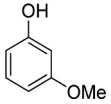	2	>99	 (76), 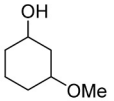 (18),  (6), Others (<1)	78	1
3	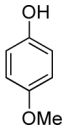	2	>99	 (56), 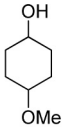 (35),  (8), Others (1)	58	9
4	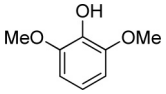	4	>99	 (70), 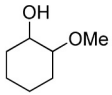 (16),  (7), Others (7)	72	7
5	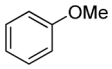	2	>99	 (61), 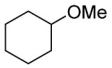 (29),  (9), Others (1)	68	6
6	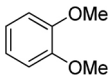	2	>99	 (55), 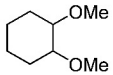 (17), 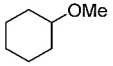 (14),  (8), Others (8)	72	6
7	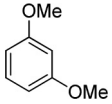	2	>99	 (46), 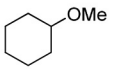 (22),  (18), 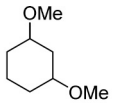 (11), Others (3)	74	7
8	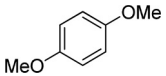	2	>99	 (43), 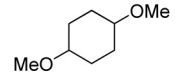 (25), 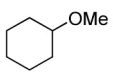 (17),  (6), Others (9)	57	11

Note: Reaction conditions: substrate (0.5 g), Ru–MnO_x/C (Ru = 5 wt%, Mn/Ru = 1; 50 mg), water (10 g), H_2 (1.5 MPa), 433 K.

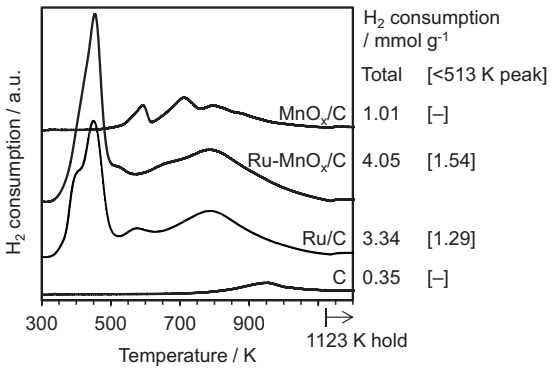

Fig. 6. H_2–TPR profiles of carbon support (Vulcan XC72), Ru/C (Ru = 5 wt%), Ru–MnO_x/C (Ru = 5 wt%, Mn/Ru = 1) and MnO_x/C (Mn = 5 wt%).

main C1 product was always methanol. The yields of cyclohexanol from these substrates (entries 2–4) were almost the same to those of the c-Ru/AC + MgO system [49]. We also applied Ru–MnO_x/C to anisole and dimethoxybenzenes which have only methoxy groups and no hydroxyl group (entries 5–8). Cyclohexane and methanol were mainly produced, indicating that demethoxylation proceeded similarly to the reactions of methoxyphenols. These selectivities were different from those of the c-Ru/AC + MgO system where total hydrogenation is the main reaction for methoxybenzenes without phenolic OH group; for example, yields of cyclohexane and methoxycyclohexane from anisole were 61% and 29%, respectively, over Ru–MnO_x/C, while they were 21% and 69% over c-Ru/AC + MgO [49]. Thus Ru–MnO_x/C is effective in selective removal of the methoxy group from aromatic substrates whether they have phenolic OH group or not, while c-Ru/AC + MgO is an effective demethoxylation catalyst only for methoxyphenols.

3.3. Catalyst characterization

Ru–MnO_x/C catalysts were characterized by TPR, XRD, TEM, CO_2–TPD and XAS. The TPR profiles of carbon black alone, fresh Ru/C, Ru–MnO_x/C and MnO_x/C are shown in Fig. 6. In the case of carbon black alone, only a weak broad signal existed above 800 K. The profile of Ru/C had strong signals between 323 and 513 K and weak signals above 513 K. The area of the low temperature peak (<513 K) of Ru/C (Ru = 0.50 mmol/g) corresponded the H_2 consumption of 1.29 mmol/g, which can be assigned to the reduction of Ru ($RuO_2 + 2H_2 \rightarrow Ru + 2H_2O$). The excess H_2 consumption (0.29 mmol/g) of this signal and the H_2 consumption of higher temperature signals were probably due to the reduction of C support catalyzed by Ru. Ru–MnO_x/C had one large signal between 323 and 513 K and broad signals above 513 K, similarly to Ru/C. The intensity of low temperature peak of Ru–MnO_x/C was stronger

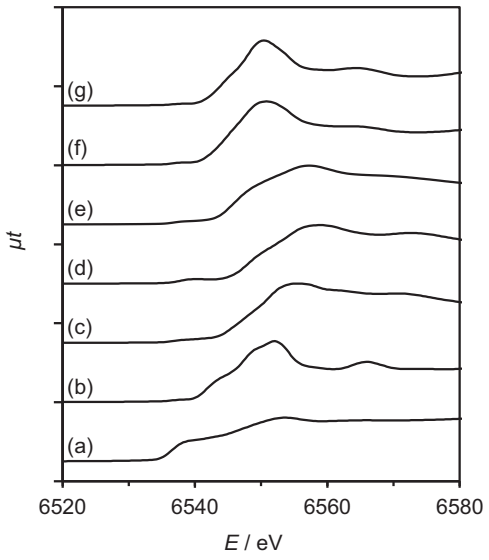

Fig. 7. Mn *K*-edge XANES spectra of Ru–MnO_x/C and reference Mn compounds. (a) Mn foil, (b) MnO, (c) Mn_2O_3, (d) MnO_2, (e) Ru–MnO_x/C after the heating treatment, (f) Ru–MnO_x/C after reduction, (g) Ru–MnO_x/C after the catalytic use.

than that of Ru/C, suggesting that Mn species are simultaneously reduced to some extent, while MnO_x/C had only signals above 550 K. The change of the average valence of Mn during the reduction of Ru–MnO_x/C was about 1.0, which was calculated by the subtraction of the amount of hydrogen consumption of Ru–MnO_x/C from that of Ru/C below 513 K. The average valence of Mn on Ru–MnO_x/C was also measured by Mn *K*-edge XANES (Fig. 7). The spectrum of Ru–MnO_x/C catalyst after heating treatment was similar to that of Mn_2O_3, and that of the reduced catalyst was similar to that of MnO. These assignments agreed with the TPR results, suggesting that the Mn species in reduced Ru–MnO_x/C is MnO.

In the XRD patterns of Ru–MnO_x/C and Ru/C after reduction, only broad peaks due to the support were observed, suggesting that Ru and Mn species are highly dispersed (Fig. S1).

Fig. 8 shows the TEM images of Ru–MnO_x/C after the reduction. Metal nanoparticles were observed, and the size was below 3 nm. The EDX analysis was conducted to determine the distribution of each metal. Although the element distribution in one particle could not be determined because of the small particle size, the element distribution of whole sample was measured. The signals from each metal were detected along the particles, indicating that MnO_x species were present nearby the metal nanoparticles of Ru.

The results of Ru *K*-edge EXAFS analysis are shown in Table 4, and the spectra are shown in Fig. S2. The spectra of Ru/C and Ru–MnO_x/C after reduction or reaction can be fitted by RuRu bond with *R* of 0.262–0.266 nm. The CN of the RuRu bond on Ru/C and

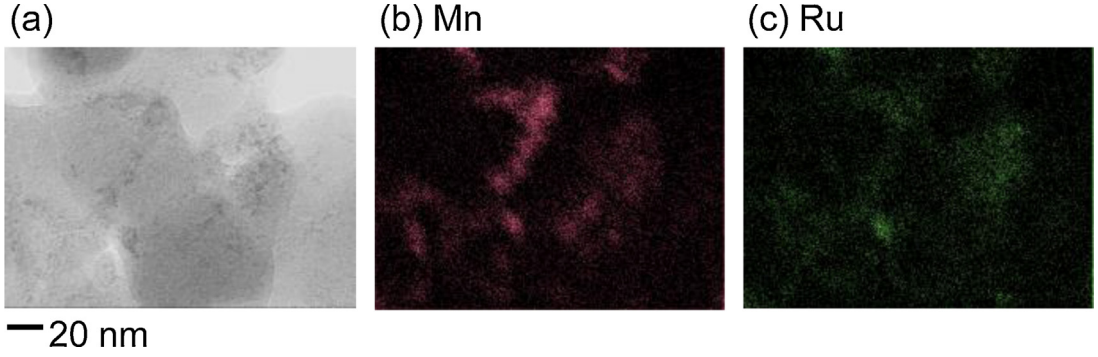

Fig. 8. (a) TEM image of Ru–MnO_x/C after reduction (Ru = 5 wt%, Mn/Ru = 1), and elemental mappings for (b) Mn and (c) Ru by EDX analysis.

Table 4
Curve fitting results of Ru *K*-edge EXAFS of Ru/C and Ru–MnO_x/C (Mn/Ru = 1).

Catalyst	Treatment	Shells	CN[a]	R (10^{-1} nm)[b]	σ (10^{-1} nm)[c]	ΔE_0 (eV)[d]	R_f(%)[e]
Ru/C	Reduction	Ru—Ru	7.5 ± 0.6	2.63 ± 0.01	0.086 ± 0.002	2.2 ± 1.1	0.71
Ru–MnO_x/C	Reaction	Ru—Ru	8.6 ± 0.5	2.66 ± 0.01	0.086 ± 0.002	2.1 ± 1.4	0.85
Ru–MnO_x/C	Reduction	Ru—Ru	6.8 ± 0.7	2. ± 0.01	0.086 ± 0.003	2.1 ± 1.6	1.2
Ru powder	–	Ru—Ru	12	2.68	0.06	0	–

[a] Coordination number.
[b] Bond distance.
[c] Debye–Waller factor.
[d] Difference in the origin of photoelectron energy between the reference and the sample.
[e] Residual factor. Fourier filtering range: 0.181–0.279 nm.

Table 5
Hydrodeoxygenation of guaiacol over Ru catalysts combined with Mn or MgO.

Entry	Catalyst	Conv. (%)	Yield (%)					Yield of C1 products (%)		pH[a]
			Cyclohexanol	Phenol	Cyclohexane	2-Methoxycyclohexanol	Others	Methanol	Methane	
1[b]	Ru–MnO_x/C	>99	81	<1	5	13	1	86	4	7.2
2	Ru/C	>99	72	<1	5	21	1	75	4	5.7
3	Ru/C + MgO	99	82	<1	6	11	1	87	2	11
4	c-Ru–MnO_x/AC	>99	76	<1	4	18	2	65	23	6.8
5[c]	c-Ru/AC	>99	66	<1	10	19	5	70	38	6.0
6[c]	c-Ru/AC + MgO	98	79	<1	7	12	1	85	3	10.8

Note: Reaction conditions: guaiacol (0.5 g), catalyst (Ru = 5 wt%, Mn/Ru = 1; 50 mg), MnO_x (0 or 50 mg), MgO (0 or 50 mg), water (10 g), H_2 (1.5 MPa), 433 K, 2 h.
[a] Measurement conditions: catalyst (50 mg), water (10 g), room temperature.
[b] Time, 4 h.
[c] Ref. [49].

Ru–MnO_x/C after reduction was 7.5 ± 0.6 and 6.8 ± 0.7, respectively, and these values were significantly lower than those of Ru metal (12). These results agreed with other characterization results including CO adsorption (CO/Ru = 0.43; Fig. 3) that highly dispersed Ru metal particles were formed. The curve fitting result for the used Ru–MnO_x/C was almost the same as that for the fresh one. Based on the above all results, the structure of Ru–MnO_x/C after reduction is determined to be composed of Ru metal particles with the size of 2–3 nm and dispersed MnO species located near the Ru particles. As shown in the previous section, small amount of Mn species is dissolved into the reaction solution in short reaction time, and the dissolved Mn returns to the solid state during the reaction. Therefore the location of Mn species during the reaction can vary during the reaction. We also conducted the reaction test using Ru/C catalyst and externally added manganese oxides (Table S4). External addition of MnO or Mn_2O_3 also increased the selectivity ratio of (cyclohexanol + phenol)/2-methoxycyclohexanol and decreased the activity. Some amount of Mn species can move from manganese oxides to the surface of Ru/C during the reaction.

CO_2–TPD profiles of Ru–MnO_x/C and Ru/C were measured to investigate the basic character of Ru–MnO_x/C (Fig. 9). Ru/C showed one desorption peak at 650 K, and Ru–MnO_x/C showed broad signals below 523 K in addition to a high-temperature peak which was similar to the peak observed in Ru/C. The total amount of CO_2 uptake of Ru–MnO_x/C, which represents the basicity, was higher than that of Ru/C. These data indicate that addition of Mn species to Ru/C created new basic sites with moderate strength on the surface of the Ru–MnO_x/C catalyst.

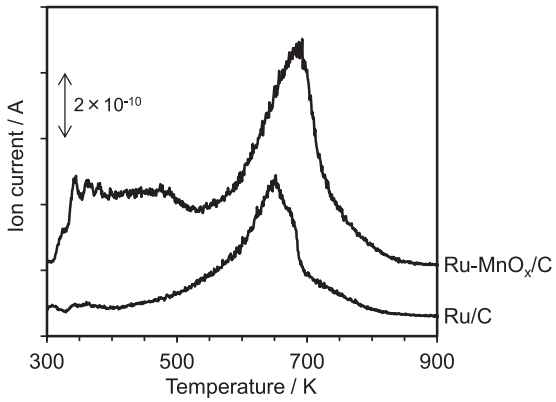

Fig. 9. CO_2–TPD profiles of Ru/C (Ru = 5 wt%) and Ru–MnO_x/C (Ru = 5 wt%, Mn/Ru = 1) after reduction.

3.4. Reaction tests related to the reaction mechanism

The effect of Mn modification was compared with that of MgO addition which was reported in our previous work [49] (Table 5). The increase in cyclohexanol yield and the decrease in 2-methoxycyclohexanol yield were similar between Mn modification and MgO addition. The difference in the cyclohexanol yield between Ru–MnO_x/C system and c-Ru/AC + MgO system in the previous study [49] is mainly due to the difference in support: The selectivity patterns to C6 products over Ru–MnO_x/C and Ru/C + MgO were similar (entries 1 and 3), and those over c-Ru-MnO_x/AC (c-Ru/AC with further impregnation of Mn) and c-Ru/AC + MgO were similar (entries 4 and 6). One difference between MnO_x modification and MgO addition was the suppression effect of methane formation: The high activity of c-Ru/AC in methane formation was almost completely suppressed by MgO addition while MnO has smaller effect.

Reactivity of possible intermediates over Ru/C, Ru-MnO_x/C and Ru/C + MgO was investigated (Table 6). Phenol was hydrogenated to cyclohexanol in higher reaction rate than guaiacol. Considering that significant amount of phenol was detected in guaiacol hydrodeoxygenation at short reaction time (Fig. 4), phenol was an intermediate of cyclohexanol from guaiacol. The reaction rate of 2-methoxycyclohexanol, catechol and 1,2-cyclohexanediol was much lower than that of guaiacol and phenol in Ru–MnO_x/C system, indicating that they were not intermediates of cyclohexanol formation. Comparison between catalysts for the same substrate showed that modification with MnO_x decreased the activity, except for 1,2-cyclohexanediol, although the number

Table 6
Hydrodeoxygenation of related substrates using Ru catalyst.

Entry	Substrate	Catalyst	Time (h)	Conv. (%)	Products (selectivity (%))	Yield of C1 products (%)	
						Methanol	Methane
1	Guaiacol	Ru–MnO_x/C	0.5	24	Cyclohexanol (38), phenol (43), 2-methoxycyclohexanol (12), cyclohexane (1), others (6)	21	<1
2		Ru/C	0.5	83	Cyclohexanol (71), phenol (3), 2-methoxycyclohexanol (17), cyclohexane (4), others (5)	72	1
3		Ru/C + MgO	0.5	56	Cyclohexanol (44), phenol (13), 2-methoxycyclohexanol (8), others (4), undetected (31)	44	<1
4	Phenol	Ru–MnO_x/C	0.5	78	Cyclohexanol (97), cyclohexanone (1), others (2)	–	–
5		Ru/C	0.5	96	Cyclohexanol (95), cyclohexane (2), cyclohexanone (1), others (2)	–	–
6		Ru/C + MgO	0.5	86	Cyclohexanol (95), benzene (3), cyclohexanone (1), others (1)	–	–
7	*trans*-2-Methoxycyclohexanol	Ru–MnO_x/C	2	5[a]	1,2-Cyclohexanediol (52), cyclohexanol (22), cyclohexane (10), others (16)	3	12
8		Ru/C	2	18[a]	1,2-Cyclohexanediol (84), cyclohexanol (15), cyclohexane (1)	3	32
9	Catechol	Ru–MnO_x/C	2	4	1,2-Cyclohexanediol (42), phenol (19), cyclohexane (18), cyclohexanol (13), others (8)	–	–
10		Ru/C	2	96	1,2-Cyclohexanediol (68), cyclohexanol (28), cyclohexane (3),	–	–
11	*trans*-1,2-Cyclohexanediol	Ru–MnO_x/C	2	18[a]	Cyclohexanol (83), cyclohexane (5), others (12)	–	–
12		Ru/C	2	10[a]	Cyclohexanol (72), cyclohexane (19), others (9)	–	–

Note: Reaction conditions: substrate (0.5 g), catalyst (each 50 mg), water (10 g), H_2 (1.5 MPa), 433 K.
[a] *Trans-cis* isomerization was excluded for calculation.

Table 7
Hydrogenolysis of cyclohexanol and methanol.

Entry	Substrate	Catalyst	Conv. (%)	Products (yield (%))
1	Cyclohexanol	Ru–MnO_x/C	2	Cyclohexane (1), C1-C5 alkanes (1)
2		Ru/C	3	Cyclohexane (2), C1-C5 alkanes (1)
3		c–Ru/AC	11	Cyclohexane (5), C1-C5 alkanes (6)
4	Methanol	Ru–MnO_x/C	10	Methane (10)
5		Ru/C	20	Methane (20)
6		c-Ru/AC	85	Methane (85)

Note: Reaction Conditions: cyclohexanol (0.5 g) or methanol (4 mmol), catalyst (Ru = 5 wt%, Mn/Ru = 1; 50 mg), water (10 g), H_2 (1.5 MPa), 433 K, 2 h.

of catalytically active site determined by CO adsorption was similar for Ru/C and Ru–MnO_x/C (Fig. 3). The reactivities of cyclohexanol and methanol were also compared between catalyst systems (Table 7). Both the support type and MnO_x modification affected the activity of those undesirable reactions, and the activity order was Ru–MnO_x/C < Ru/C « c-Ru/AC. The c-Ru/AC catalyst showed considerable activity in the cracking reaction (entry 3), which agree with the high methane yield in guaiacol reduction over c-Ru/AC (Tables 1 and 5).

The dependences of the catalysis on the reaction conditions are investigated and shown in Fig. 10 (hydrogen pressure and temperature), Fig. S3 (catalyst amount) and Fig. S4 (substrate amount and the reaction in ethanol). The reaction proceeded faster under higher hydrogen pressure. Higher reaction temperature and lower hydrogen pressure conditions were favorable for demethoxylation. 2-Methoxycyclohexanol production was suppressed by these conditions, while cyclohexane formation was slightly enhanced by higher reaction temperature. These trends on the reaction parameters were similar to those of c-Ru/AC + MgO system [49]. Varying the catalyst amount hardly changed the selectivity ratio of (phenol + cyclohexanol)/(2-methoxycyclohexanol), while the selectivity to cyclohexane was gradually increased by decreasing the catalyst amount. Too low substrate concentration slightly decreased the selectivity ratio of (phenol + cyclohexanol)/(2-methoxycyclohexanol). Ethanol solvent was much inferior to water solvent in terms of both activity and selectivity to monooxygenates (cyclohexanol + phenol).

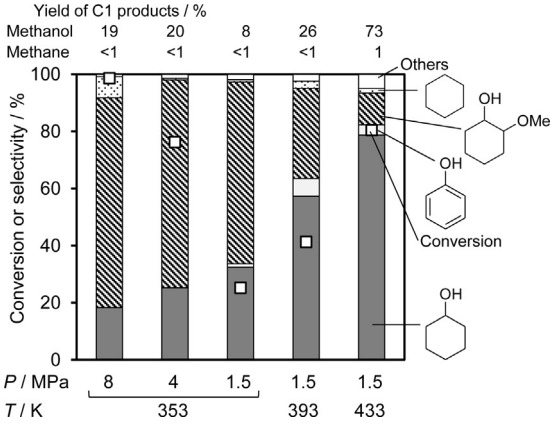

Fig. 10. Reaction conditions dependence of the hydrodeoxygenation of guaiacol over Ru–MnO_x/C. Reaction conditions: guaiacol (0.5 g), Ru–MnO_x/C (50 mg, Ru 5 wt%, Mn/Ru = 1), water (10 g), 2 h.

3.5. Reaction mechanism

Here we discuss the reaction mechanism. In our previous work (the c-Ru/AC + MgO system) [49], we proposed the reaction network for guaiacol hydrodeoxygenation: First guaiacol was partially hydrogenated to dihydroguaiacol. Then two reactions could proceed from dihydroguaiacol: further hydrogenation to 2-

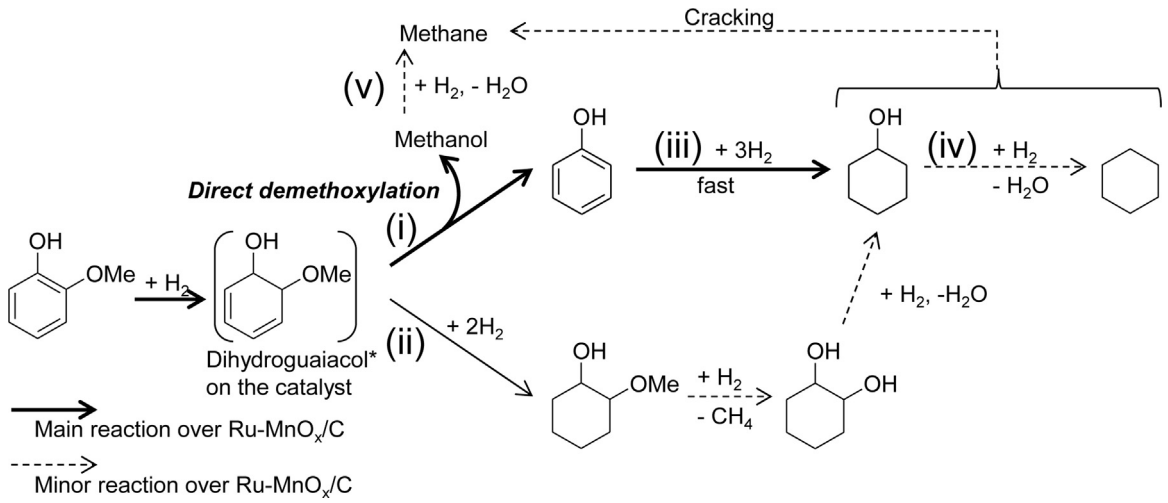

Fig. 11. Proposed reaction pathway of hydrodeoxygenation of guaiacol over Ru–MnO_x/C. *The structure shown here for dihydroguaiacol is one of the possible structures. Dihydroguaiacol was not detected in the liquid phase.

methoxycyclohexanol and the removal of methanol to phenol. Phenol was readily hydrogenated to cyclohexanol. Hydrodeoxygenation of saturated compounds is slow, and the main products are cyclohexanol, 2-methoxycyclohexanol and methanol. Lower hydrogen pressure and higher reaction temperature increases the selectivity to cyclohexanol by increasing the relative rate of methanol removal to hydrogenation of dihydroguaiacol.

Because the Ru–MnO_x/C system and the c-Ru/AC + MgO system showed similar properties such as dependency on reaction conditions and low reactivities of saturated compounds, we assume essentially the same mechanism for Ru–MnO_x/C (Fig. 11). In the literature, other reaction mechanisms of noble-metal-catalyzed guaiacol reduction to mono-oxygenated compounds have been proposed: (a) Demethylation of guaiacol to catechol followed by dehydroxylation to phenol [26,30,44]; (b) total hydrogenation of guaiacol to 2-methoxycyclohexanol followed by demethoxylation to cyclohexanol [47,50,53]; (c) partial hydrogenation of guaiacol to 2-methoxycyclohexanone followed by demethoxylation to cyclohexanone [39,41,52]. The mechanism (a) can be ruled out because catechol is not reactive over Ru–MnO_x/C, and the mechanisms (b) and (c) can be ruled out because they do not involve phenol as an intermediate. The much lower temperature of this system than the literature ones may cause the reaction in this different path.

In this mechanism, the relative rate of the demethoxylation (step (i)) to hydrogenation (step (ii)) of dihydroguaiacol critically determines the selectivity to cyclohexanol. In the case of c-Ru/AC + MgO system, stabilization of acidic intermediate (phenol) by the basic media was proposed to be a key to high cyclohexanol yield, because anisole and dimethoxybenzene were not readily demethoxylated [49]. However, this explanation cannot be applied to this Ru–MnO_x/C catalyst because demethoxylation of these substrates actually proceeded over Ru–MnO_x/C. In fact, the basicity of Ru–MnO_x/C is much weaker than MgO as shown by the pH values of the aqueous mixture (Table 5). It is likely that basicity is not the critical factor in the higher demethoxylation selectivity of Ru–MnO_x/C than Ru/C, while the basicity of Ru–MnO_x/C can have a role in suppressing another side reaction, namely cyclohexane formation, as discussed later.

Here we pay attention to the lower activity of Ru–MnO_x/C than that of Ru/C in C=C hydrogenation as shown in Table 6 (entries 1–6). If the rate of step (i) is constant, lower rate of step (ii) leads to higher selectivity to demethoxylation products. In fact, among oxide-supported Ru catalysts, the catalysts with lower activity tended to show higher selectivity to demethoxylation products (cyclohexanol, phenol and cyclohexane), as discussed in Section 3.1. On the other hand, simply decreasing the catalyst amount did not increase the selectivity to demethoxylation products (Fig. S3). This behavior can be explained by that the dihydroguaiacol intermediate is not present as free molecules but adsorbed on the catalytically active site. The fact that dihydroguaiacol was not detected at all also agreed with this idea.

The hydrodeoxygenation of cyclohexanol to cyclohexane (step (iv)), that of methanol to methane (step (v)) and cracking reactions are side-reactions that decrease the yield of cyclohexanol or methanol. These side reactions were suppressed by choosing appropriate supports, MnO_x modification or MgO addition. The step (iv) was known to proceed via acid-catalyzed dehydration to cyclohexene and subsequent hydrogenation. Active carbon has more number of acidic groups than carbon blacks, and therefore the use of carbon black instead of active carbon can decrease the activity for step (iv). MnO_x and MgO are basic species, and MnO_x modification or MgO addition can decrease the activity of acidic sites, decreasing the reaction rate of step (iv). Cracking reaction and methane formation from methanol are typically catalyzed by noble metal surface [68,69]. The decrease in the activity of cracking and methane formation from methanol may be due to the modification of Ru surface with Mn or Mg species.

4. Conclusions

Selective production of cyclohexanol and methanol from guaiacols were achieved by using Ru–MnO_x catalyst using carbon black support (Ru–MnO_x/C). The catalyst was reusable without significant loss on the catalytic performance and was easier to handle than commercial c-Ru/AC + MgO system which was reported earlier. Other methoxybenzenes such as 2,6-dimethoxyphenols and anisole were also converted to demethoxylated saturated compounds such as cyclohexanol and cyclohexane, while commercial c-Ru/AC + MgO system does not readily demethoxylate these methoxybenzenes without phenolic OH group. In the reduced Ru–MnO_x/C catalyst, MnO species were located nearby the highly dispersed metal nanoparticles of Ru. The reaction of guaiacol is suggested to proceed through demethoxylation of partially hydrogenated guaiacol (dihydroguaiacol) to phenol followed by hydrogenation to cyclohexanol. Total hydrogenation of dihydroguaiacol to 2-methoxycyclohexanol also proceeds in parallel. The slower reaction rate for hydrogenation of aromatic ring over Ru–MnO_x/C than Ru/C, which was derived from addition of Mn

species, increases the relative rate of demethoxylation to total hydrogenation, resulting in higher yield of demethoxylated products. The choice of support is essential in suppressing undesirable reactions such as demethylation, over-hydrodeoxygenation and hydrocracking, and carbon black is one of the best supports. Modification of Ru metal with MnO species is also effective in suppressing these side-reactions.

Acknowledgments

This study is supported by JSPS KAKENHI grant number 26249121 and 15K06564. We also acknowledge the Technical Division in the School of Engineering in Tohoku University for TEM measurements.

Appendix A. Supplementary data

Supplementary data associated with this article can be found, in the online version, at http://dx.doi.org/10.1016/j.apcatb.2015.09.021.

References

[1] G.W. Huber, S. Iborra, A. Corma, Chem. Rev. 106 (2006) 4044–4098.
[2] A.J. Ragauskas, C.K. Williams, B.H. Davison, G. Britovsek, J. Cairney, C.A. Eckert, W.J. Frederic Jr., J.P. Hallett, D.J. Leak, C.L. Liotta, J.R. Mielenz, R. Murphy, R. Templer, T. Tschaplinski, Science 311 (2006) 484–489.
[3] A.-L. Marshall, P.J. Alaimo, Chem. Eur. J. 16 (2010) 4970–4980.
[4] G.W. Huber, A. Corma, Angew. Chem. Int. Ed. 46 (2007) 7184–7201.
[5] H. Wang, J. Male, Y. Wang, ACS Catal. 3 (2013) 1047–1070.
[6] J. Zakzeski, P.C.A. Bruijnincx, A.L. Jongerius, B.M. Weckhuysen, Chem. Rev. 110 (2010) 3552–3599.
[7] D.J. Nowakowski, A.V. Bridgwater, D.C. Elliott, D. Meier, P. de Wild, J. Anal. Appl. Pyrol. 88 (2010) 53–72.
[8] R.N. Olcese, M. Bettahar, D. Petitjean, B. Malaman, F. Giovanella, A. Dufour, Appl. Catal. B: Environ. 115–116 (2012) 63–73.
[9] S. Van den Bosch, W. Schutyser, R. Vanholme, T. Driessen, S.-F. Koelewijn, T. Renders, B. De Meester, W.J.J. Huijgen, W. Dehaen, C.M. Courtin, B. Lagrain, W. Boerjan, B.F. Sels, Energy Environ. Sci. 8 (2015) 1748–1763.
[10] Y. Nakagawa, K. Tomishige, Catal. Sci. Technol. 1 (2011) 179–190.
[11] K. Tomishige, M. Tamura, Y. Nakagawa, Chem. Rec. 14 (2014) 1041–1054.
[12] A.M. Ruppert, K. Weinberg, R. Palkovits, Angew. Chem. Int. Ed. 51 (2012) 2564–2601.
[13] Y. Nakagawa, M. Tamura, K. Tomishige, ACS Catal. 3 (2013) 2655–2668.
[14] Y. Nakagawa, S. Liu, M. Tamura, K. Tomishige, ChemSusChem 8 (2015) 1114–1132.
[15] Q. Bu, H. Lei, A.H. Zacher, L. Wang, S. Ren, J. Liang, Y. Wei, Y. Liu, J. Tang, Q. Zhang, R. Ruan, Bioresour. Technol. 124 (2012) 470–477.
[16] T.N. Pham, D. Shi, D.E. Resasco, Appl. Catal. B: Environ. 145 (2014) 10–23.
[17] V.N. Bui, D. Laurenti, P. Afanasiev, C. Geantet, Appl. Catal. B: Environ. 101 (2011) 239–245.
[18] E. Laurent, B. Delmon, Appl. Catal. A: Gen. 109 (1994) 77–96.
[19] A. Pinheiro, D. Hudebine, N. Dupassieux, C. Geantet, Energy Fuels 23 (2009) 1007–1014.
[20] D.C. Elliott, Energy Fuels 21 (2007) 1792–1815.
[21] I.D. Mora, E. Méndez, L.J. Duarte, S.A. Giraldo, Appl. Catal. A: Gen. 474 (2014) 59–68.
[22] H.Y. Zhao, D. Li, P. Bui, S.T. Oyama, Appl. Catal. A: Gen. 391 (2011) 305–310.
[23] S.-K. Wu, P.-C. Lai, Y.-C. Lin, H.-P. Wan, H.-T. Lee, Y.-H. Chang, ACS Sustain. Chem. Eng. 1 (2013) 349–358.
[24] A.L. Jongerius, R.W. Gosselink, J. Dijkstra, J.H. Bitter, P.C.A. Bruijnincx, B.M. Weckhuysen, ChemCatChem 5 (2013) 2964–2972.
[25] I.T. Ghampson, C. Sepúlveda, R. Garcia, B.G. Frederick, M.C. Wheeler, N. Escalona, W.J. DeSisto, Appl. Catal. A: Gen. 413–414 (2012) 78–84.
[26] J. Chang, T. Danuthai, S. Dewiyanti, C. Wang, A. Borgna, ChemCatChem 5 (2013) 3041–3049.
[27] R.K.M.R. Kallury, W.M. Restivo, T.T. Tidwell, D.G.B. Boocock, A. Crimi, J. Douglas, J. Catal. 96 (1985) 535–543.
[28] C. Sepúlveda, K. Leiva, R. García, L.R. Radovic, I.T. Ghampson, W.J. DeSisto, J.L.G. Fierro, N. Escalona, Catal. Today 172 (2011) 232–239.
[29] J. Filley, C. Roth, J. Mol. Catal. A: Chem. 139 (1999) 245–252.
[30] J. Sun, A.M. Karim, H. Zhang, L. Kovarik, X.S. Li, A.J. Hensley, J.-S. McEwen, Y. Wang, J. Catal. 306 (2013) 47–57.
[31] M.V. Bykova, O.A. Bulavcchenko, D.Y. Ermakov, M.Y. Lebedev, V.A. Yakovlev, V.N. Parmon, Catal. Ind. 3 (2011) 15–22.
[32] W. Song, Y. Liu, E. Baráth, C. Zhao, J.A. Lercher, Green Chem. 17 (2015) 1204–1218.
[33] J.E. Peters, J.R. Carpenter, D.C. Dayton, Energy Fuels 29 (2015) 909–916.
[34] W. Schutyser, S. Van den Bosch, J. Dijkmans, S. Turner, M. Meledina, G. Van Tendeloo, D.P. Debecker, B.F. Sels, ChemSusChem 8 (2015) 1805–1818.
[35] C. Zhao, J.A. Lercher, Angew. Chem. Int. Ed. 51 (2012) 5935–5940.
[36] K.L. Deutsch, B.H. Shanks, Appl. Catal. A: Gen. 447–448 (2012) 144–150.
[37] T. Mochizuki, S.-Y. Chen, M. Toba, Y. Yoshimura, Appl. Catal. B: Environ. 146 (2014) 237–243.
[38] K. Leiva, N. Martinez, C. Sepulveda, R. García, C.A. Jiménez, D. Laurenti, M. Vrinat, C. Geantet, J.L.G. Fierro, I.T. Ghampson, N. Escalona, Appl. Catal. A: Gen. 490 (2015) 71–79.
[39] C. Zhao, J. He, A.A. Lemonidou, X. Li, J.A. Lercher, J. Catal. 280 (2011) 8–16.
[40] Y.-K. Hong, D.-W. Lee, H.-J. Eom, K.-Y. Lee, Appl. Catal. B: Environ. 150–151 (2014) 438–445.
[41] Y.-C. Lin, C.-L. Li, H.-P. Wan, H.-T. Lee, C.-F. Liu, Energy Fuels 25 (2011) 890–896.
[42] H. Ohta, H. Kobayashi, K. Hara, A. Fukuoka, Chem. Commun. 47 (2011) 12209–12211.
[43] T. Nimmanwudipong, R.C. Runnebaum, D.E. Block, B.C. Gates, Energy Fuels 25 (2011) 3417–3427.
[44] M.Á. González-Borja, D.E. Resasco, Energy Fuels 25 (2011) 4155–4162.
[45] T. Nimmanwudipong, C. Aydin, J. Lu, R.C. Runnebaum, K.C. Brodwater, N.D. Browning, D.E. Block, B.C. Gates, Catal. Lett. 142 (2012) 1190–1196.
[46] A.K. Deepa, P.L. Dhepe, ChemPlusChem 79 (2014) 1573–1583.
[47] M. Hellinger, H.W.P. Carvalho, S. Baier, D. Wang, W. Kleist, J.-D. Grunwaldt, Appl. Catal. A: Gen. 490 (2015) 181–192.
[48] S. Boonyasuwat, T. Omotoso, D.E. Resasco, S.P. Crossley, Catal. Lett. 143 (2013) 783–791.
[49] Y. Nakagawa, M. Ishikawa, M. Tamura, K. Tomishige, Green Chem. 16 (2014) 2197–2203.
[50] M.-Y. Chen, Y.-B. Huang, H. Pang, X.-X. Liu, Y. Fu, Green Chem. 17 (2015) 1710–1717.
[51] Y.-B. Huang, L. Yan, M.-Y. Chen, Q.-X. Guo, Y. Fu, Green Chem. 17 (2015) 3010–3017.
[52] A. Gutierrez, R.K. Kaila, M.L. Honkela, R. Slioor, A.O.I. Krause, Catal. Today 147 (2009) 239–246.
[53] C.R. Lee, J.S. Yoon, Y.-W. Suh, J.-W. Choi, J.-M. Ha, D.J. Suh, Y.-K. Park, Catal. Commun. 17 (2012) 54–58.
[54] T. Miyazawa, S. Koso, K. Kunimori, K. Tomishige, Appl. Catal. A: Gen. 318 (2007) 244–251.
[55] Y.J. Mergler, A. van Aalst, J. van Delft, B.E. Nieuwenhuys, J. Catal. 161 (1996) 310–318.
[56] J.W. Cook, D.E. Sayers, J. Appl. Phys. 52 (1981) 5024–5031.
[57] K. Okumura, J. Amano, N. Yasunobu, M. Niwa, J. Phys. Chem. B 104 (2000) 1050–1057.
[58] K. Okumura, S. Matsumoto, N. Nishiaki, M. Niwa, Appl. Catal. B: Environ. 40 (2003) 151–159.
[59] K. Tomishige, K. Asakura, Y. Iwasawa, J. Catal. 147 (1994) 70–80.
[60] N. Ota, M. Tamura, Y. Nakagawa, K. Okumura, K. Tomishige, Angew. Chem. Int. Ed. 54 (2015) 1897–1900.
[61] Y. Amada, N. Ota, M. Tamura, Y. Nakagawa, K. Tomishige, ChemSusChem 7 (2014) 2185–2192.
[62] M. Tamura, R. Tamura, Y. Takeda, Y. Nakagawa, K. Tomishige, Chem. Commun. 50 (2014) 6656–6659.
[63] Y. Takeda, Y. Nakagawa, K. Tomishige, Catal. Sci. Technol. 2 (2012) 2221–2223.
[64] M. Chia, Y.J. Pagán-Torres, D. Hibbitts, Q. Tan, H.N. Pham, A.K. Datye, M. Neurock, R.J. Davis, J.A. Dumesic, J. Am. Chem. Soc. 133 (2011) 12675–12689.
[65] R. Arundhathi, T. Mizugaki, T. Mitsudome, K. Jitsukawa, K. Kaneda, ChemSusChem 6 (2013) 1345–1347.
[66] S.M. Santos, A.M. Silva, E. Jordão, M.A. Fraga, Catal. Commun. 5 (2004) 377–381.
[67] T. Miyake, T. Makino, S. Taniguchi, H. Watanuki, T. Niki, S. Shimizu, Y. Kojima, M. Sano, Appl. Catal. A: Gen. 364 (2009) 108–112.
[68] G.B. McVicker, M. Daage, M.S. Touvelle, C.W. Hudson, D.P. Klein, W.C. Baird Jr., B.R. Cook, J.G. Chen, S. Hantzer, D.E.W. Vaughan, E.S. Ellis, O.C. Feeley, J. Catal. 210 (2002) 137–148.
[69] D.W. McKee, Trans. Faraday Soc. 64 (1968) 2200–2212.